HHS Public Access

Author manuscript

Nat Microbiol. Author manuscript; available in PMC 2016 November 27.

Published in final edited form as:

Nat Microbiol. ; 1(7): 16084. doi:10.1038/nmicrobiol.2016.84.

Shigella flexneri suppresses NF-kB activation by inhibiting linear ubiquitin chain ligation

Maarten F. de Jong[1], **Zixu Liu**[1], **Didi Chen**[1], and **Neal M. Alto**[1,*]

[1]Department of Microbiology, University of Texas Southwestern Medical Center, Dallas, TX 75390, USA

Abstract

The Linear Ubiquitin chain Assembly Complex (LUBAC) is a multimeric E3 ligase that catalyzes M1- or linear ubiquitination of activated immune receptor signaling complexes (RSCs). While mutations that disrupt linear ubiquitin assembly lead to complex disease pathologies including immunodeficiency and autoinflammation in both humans and mice, microbial toxins that target LUBAC function have not yet been discovered. Here, we report the identification of two homologous *Shigella flexneri* Type III Secretion System (T3SS) effector E3 ligases IpaH1.4 and IpaH2.5 that directly interact with LUBAC subunit HOIL-1L (*RBCK1*) and conjugate K48-linked ubiquitin chains to the catalytic RING-between-RING domain of HOIP (*RNF31*). Proteasomal degradation of HOIP leads to irreversible inactivation of linear ubiquitination and blunting of NF-κB nuclear translocation in response to TNF, IL-1β, and pathogen associated molecular patterns (PAMPs). Loss of function studies in mammalian cells in combination with bacterial genetics explains how *Shigella* evades a broad spectrum of immune surveillance systems by cooperative inhibition of receptor ubiquitination, and reveals the critical importance of LUBAC in host defense against pathogens.

The Linear Ubiquitin chain Assembly Complex (LUBAC) is a multimeric E3 ligase composed of two accessory subunits HOIL-1L (RBCK1) and SHARPIN, and a catalytic subunit HOIP (RNF31). Recruitment of LUBAC to activated cytokine- or Pattern Recognition Receptors (PRRs)[1-3] results in the ligation of RIPK1 and NEMO (IKKγ) with methionine 1 (M1)-linked linear ubiquitin (Ub) chains[4]. This ubiquitination event is crucial for activation of transcription factors NF-κB and AP-1 that induce rapid gene expression in response to microbial infection[2,4-7]. Because of the ubiquitous requirement of M1-Ub in numerous cytokine signaling pathways, humans lacking functional LUBAC exhibit severe autoinflammatory diseases and are especially vulnerable to pyogenic bacterial infections including life-threatening enteroinvasive *Escherichia coli*[8,9]. While recent studies have

---

*Correspondence to: neal.alto@utsouthwestern.edu.

Contributions

M.F.D.J. and N.M.A. were responsible for study design, the analysis and interpretation of data, and for writing the manuscript. M.F.D.J. performed and analyzed the experiments. Z.L. and D.C. developed essential assays systems.

Competing financial Interests

The authors declare no competing financial interests

elucidated many of the structural and biochemical properties of LUBAC function, it remains unclear how pathogens avoid immunological detection propagated by M1-Ub chain ligation.

Gram-negative bacteria including *Yersinia*, *E. coli*, *Salmonella* and *Shigella* utilize Type III Secretion Systems (T3SS) to dampen the innate immune response to infection[10]. These bacteria secrete between 10 and 50 effector proteins, many of which have unknown functions. Identifying substrates targeted by individual effector proteins has been confounded by the functional redundancy found within the repertoire of secreted effectors and by the complexity of host molecules that are assembled at activated immune receptors (e.g. TNF-R1, IL-1R, TLR). Thus, new model systems are needed to elucidate the immune evasion strategies employed by these microbial pathogens. Here, we focused on mechanisms of innate immune evasion by *Shigella flexneri*, an enteroinvasive pathogen that infects an estimated 165 million people, resulting in more than one million deaths annually[11]. *Shigella* spp., are closely related to enteroinvasive *E. coli* (EIEC)[12]. These pathogens invade intestinal epithelial cells and encode multiple T3SS effector proteins on a large virulence plasmid, of which some have been shown to target host defense systems[12-17]. Additionally, we sought to identify novel inhibitors of cytokine signaling by developing a simplified host cell system to examine effector mechanisms for NF-κB suppression (Fig. 1a)

Here, we show that the *S. flexneri* E3 ligase effectors IpaH1.4 and IpaH2.5 interact with HOIL-1L and HOIP subunits of LUBAC and direct K48-linked ubiquitination and proteasomal destruction of HOIP. While LUBAC destruction is sufficient to suppress immune responses induced by TNF, elimination of both M1- and K63-linked Ub chains are required to inhibit diverse receptors, including PRRs and IL-1R during *Shigella* infection. Collectively, these results (1) establish an irreversible mechanism of host immune suppression through proteasome-dependent elimination of M1-linked linear ubiquitination, (2) reveal the requirement for cooperativity among T3SS effectors, and (3) provide alternative avenues for interrogating immune receptor activation in combined immunodeficiency and autoinflammatory diseases associated with LUBAC dysfunctions.

Results

Shigella modulators of innate immune signaling pathways

A simplified cell-based assay was used to characterize the anti-immunological function of *Shigella* T3SS effector proteins. As shown in Figure 1a, ectopic expression of specific TNF-RSC components TRAF2, TAK1/Tab2, or LUBAC induced NF-κB mediated transcriptional responses (Fig. 1a and b). Consistent with previous studies, NF-κB activation by expression of TRAF2 E3 ligase was potently inhibited by *Shigella* OspI (Fig. 1b), a T3SS effector protein that deamidates Ubc13 required for TRAF2 directed K63-linked Ub chain conjugation of TNF-RSC[17]. We also found that OspZ, a T3SS effector that inactivates the TAK/Tab kinase complex, inhibited TRAF2 mediated NF-κB activation. These data are consistent with OspZ induced methylation of the high-affinity K63-Ub binding NZF domain of Tab2[18,19]. Thus, *Shigella* can suppress signaling through K63-linked Ub chains at the level of receptor K63-ubiquitylation and/or K63-Ub mediated recruitment of TAK/Tab.

Interestingly, we also observed a partial reduction of TRAF2 induced NF-κB activation in cells expressing IpaH1.4, but not other IpaH family members including IpaH9.8 (Fig. 1b). In contrast, IpaH1.4 did not inhibit NF-κB activation in cells expressing TAK1/Tab2 (Fig. 1b). IpaH1.4 therefore targets a signaling component that depends on formation of K63-linked Ub chains, but that does not depend on downstream phosphorylation steps in the pathway (Fig. 1a). The Linear Ubiquitin chain Assembly Complex (LUBAC) is recruited to the TNF-RSC through binding to K63-linked Ub chains and conjugates M1-linked Ub chains to TNF-RSC (Fig. 1a)[2,20]. IpaH1.4 potently inhibited NF-κB stimulation by LUBAC, whereas OspI and OspZ had little effect (Fig. 1b).

IpaH1.4 belongs to a large family of bacterial E3 ligases characterized by a highly variable NH_2-terminal Leucine Rich Repeat (LRR) domain and a nearly identical COOH-terminal catalytic domain (Supplementary Fig. 1a)[21,22]. LUBAC signaling was inhibited by both IpaH1.4 and IpaH2.5, which share 98% sequence homology[14], but not other family members including IpaH4.5, IpaH7.8 and IpaH9.8 that share less than 80% homology (Supplementary Fig. 1b). The E3 ligase activity of IpaH1.4/2.5[21,22] was necessary for inhibiting LUBAC stimulated NF-κB activation (Supplementary Fig. 1c). Evaluation of experiments in Figure 1b also revealed a consistent downregulation of LUBAC-mediated NF-κB by *Shigella* kinase OspG. However, we found the kinase activity was unnecessary for LUBAC inhibition (Supplementary Fig. 1c) and an unbiased yeast two-hybrid screen failed to identify OspG substrates beyond its established activators Ub and Ube2L3 (UbcH7) E2-conjugating enzyme (Supplementary Fig. 2a)[16,23,24]. It is therefore likely that OspG inhibits LUBAC through non-specific sequestration of Ube2L3~Ub machinery required for linear ubiquitination under these experimental conditions[25,26]. Taken together, we confirmed previous work on *Shigella* effector proteins OspI and OspZ that target K63-linked Ub chains and demonstrate that *Shigella* may require additional effector proteins, and particularly IpaH1.4/2.5, to target M1-linked Ub chains to effectively suppress host defense mechanisms.

IpaH1.4/2.5 directly interacts with LUBAC

To elucidate the molecular mechanism of IpaH1.4/2.5 targeting of LUBAC, an unbiased yeast two-hybrid screen for IpaH2.5 substrates identified the ubiquitin-like domain (UBL) of the LUBAC subunit HOIL-1L (Supplementary Fig. 2a). IpaH2.5 also bound to full-length HOIL-1L in this assay (Supplementary Fig. 2b), suggesting a direct mechanism of LUBAC regulation. The UBL domain of HOIL-1L is required for LUBAC assembly through interaction with the UBA domain of HOIP[25,26]. We then asked if IpaH1.4/2.5 directly interacts with intact LUBAC, and if so, what protein regions are necessary and sufficient for substrate recognition? A “mini-LUBAC” was generated by mixing a fragment of HOIL-1L encompassing the UBL domain (HOIL-$1L_{UBL}$, residues 1-134) with a GST-tagged fragment of HOIP encompassing the UBA and catalytic Ring-Between-Ring (RBR) domain ($HOIP_{UBA-RBR}$, residues 557-1072). Mini-LUBAC precipitated recombinant MBP-tagged IpaH2.5, but not MBP control (Fig. 1c, lanes 7-8), showing that the *Shigella* effector proteins directly interact with the pre-assembled E3 ligase complex. Unexpectedly, $HOIP_{UBA-RBR}$ precipitated IpaH2.5 even in the absence of HOIL-$1L_{UBL}$ (Fig. 1c, lane 6), revealing an additional interaction site for IpaH1.4/2.5 in HOIP.

Cell based studies confirmed the interaction between full-length HOIP and catalytically inactive IpaH1.4/2.5$_{C368S}$, but not other IpaH family members (Supplementary Fig. 2c-e). Truncation analysis (Fig. 1d) revealed the binding-site on HOIP, encompassing the HOIP UBA domain (e.g. HOIP$_{\Delta C2}$) that binds HOIL-1L and the region between the UBA-domain and the catalytic RBR domain (e.g. HOIP$_{\Delta N2}$) (Fig. 1e, arrows). The combination of UBA and RBR consistently yielded the greatest interaction with IpaH2.5 (Fig. 1e, lane 4), further confirming the interaction between two E3 ligases of different species.

IpaH1.4/2.5 mediates proteasomal degradation of HOIP

LUBAC exists as a heterodimer, or heterotrimer, composed of HOIL-1L and/or SHARPIN in complex with the catalytic subunit HOIP (LUBAC I, II, and III). Co-expression of IpaH1.4/2.5 with each of the three LUBAC forms in HeLa cells revealed a significant reduction in HOIP protein levels, with no corresponding reduction in either HOIL-1L or SHARPIN (Fig. 2a). Mutant IpaH2.5$_{C368S}$ lacking E3 ligase function did not reduce HOIP protein stability. In addition, IpaH4.5, 7.8, and 9.8 did not target HOIP or any LUBAC subunit for degradation (Fig. 2a). HOIP protein stability was rescued in IpaH1.4 or IpaH2.5 expressing cells treated with proteasome inhibitor MG132, showing that IpaH1.4/2.5 mediated HOIP degradation is proteasome dependent (Fig 2b). Finally, we identified residues 687-761 encompassing RING1 of the catalytic RBR domain[27] as the minimal HOIP fragment destabilized in cells expressing IpaH2.5 (Fig. 2c). RING1 is adjacent to the IpaH2.5 binding site on HOIP (Fig. 1d), indicating that IpaH1.4/2.5 directly interacts with LUBAC and targets HOIP for ubiquitin-mediated proteasomal degradation (Fig. 2d, illustration).

We performed *Shigella* infection experiments to test the ability of IpaH1.4/2.5 to degrade endogenous HOIP in a human intestinal epithelial cell line (CaCo-2). An infection rate of ~50% could be achieved without appreciable cell death (Supplementary Fig. 3), which set the limitation on the total HOIP degradation that could be monitored in bulk biochemical experiments. As shown in Figure 2e, WT *Shigella* reduced endogenous HOIP by more than 50% (consistent with the rate of bacterial infection), but not HOIL-1L or β-actin control. HOIP degradation was not observed during infection with the *ShigellaΔipaH1.4/2.5* strain and analysis of single mutations revealed IpaH1.4 is the essential bacterial E3 ligase necessary for targeting LUBAC in this cellular model of infection (Fig. 2e). The varying promoter sequences upstream of *ipaH1.4* and *ipaH2.5* genes (52.0% identity), but nearly identical coding sequences (98.9% identity) suggest that although *ipaH1.4* and *ipaH2.5* encode identical proteins, expression may vary depending on conditions encountered by *Shigella* during infection (Supplementary Fig. 4).

We were unable to complement the *ShigellaΔipaH1.4* strain with an arabinose inducible copy of *ipaH1.4* or *ipaH2.5* encoded on a plasmid. To then determine if IpaH1.4/2.5 targets LUBAC function at protein levels secreted by bacterial pathogens, we engineered an attenuated *Listeria monocytogenes* (*Lm*) strain to secrete IpaH2.5 during intracellular invasion (Supplementary Fig. 5a). Both *Lm* and *Shigella* have very similar intracellular lifestyles, yet *Lm* does not encode IpaH homolog or induce HOIP degradation. We observed dose and time dependent degradation of endogenous HOIP in U2OS cells infected with

Lm::ipaH2.5, but not infected with WT or *IpaH2.5*$_{C368S}$ secreting strains (Supplementary Fig. 5b-d). These data further confirm that IpaH1.4/2.5 specifically targets HOIP during infection.

IpaH1.4/2.5 ubiquitinates the RBR domain of HOIP *in vitro*

Next, we reconstituted the ubiquitination reaction to determine if IpaH1.4/2.5 directly modifies LUBAC. 6X-Histidine tagged Flag-SHARPIN was co-expressed with Myc-HOIP and Flag-HOIL-1L in HeLa cells and the intact LUBAC-III was purified by Ni-NTA affinity chromatography (Fig. 3a). LUBAC-III was then mixed with recombinant human UbE1(E1), UbcH5b(E2), Flag-Ub, and ATP (Fig. 3b). Addition of either recombinant IpaH1.4 or IpaH2.5 induced a large (over 150 kDa) and time-dependent shift in HOIP mobility compared to untreated samples (Fig. 3c, lanes 1-2; Supplementary Fig. 6a and b). This mobility shift depended on both catalytic Cys368 in IpaH2.5 (Fig. 3c, lane 7) and the presence of the E1 ubiquitin activating enzyme UbE1 (lane 8) indicating that IpaH1.4/2.5 directly ubiquitinates HOIP. The isolated E3 ligase domain (NEL, residues 265-575) did not ubiquitinate HOIP, suggesting that similar to IpaH family member SspH1 from *Salmonella*[28], the LRR domain of IpaH1.4/2.5 defines its substrate selectivity (lane 6). Consistent with this notion, IpaH4.5, IpaH7.8, and IpaH9.8 that encode highly variable LRRs yet identical E3 ligase domains were unable to catalyze HOIP ubiquitination (lanes 3-5). Finally, neither HOIL-1L nor SHARPIN were modified by IpaH1.4/2.5 (Supplementary Fig. 6a), demonstrating that HOIP is the primary target of the bacterial E3 ligase machinery.

Mass Spectrometry analysis identified K735, K783 and K875 of HOIP as the primary residues ubiquitinated by IpaH2.5 *in vitro* (Fig. 3d, Supplementary Fig. 7). K735 is located in the RING1 domain, K783 in the IBR domain, and K875 in the RING2 domain of HOIP. These sites of modification are in agreement with the IpaH2.5 binding site near RING1 (Fig. 1d), the RING1 domain itself being required for degradation in cells (Fig. 2d), and the RBR domain being directly ubiquitinated by IpaH1.4/2.5 *in vitro* (Supplementary Fig. 6c, lanes 1-3). IpaH2.5 induced cellular degradation (Fig. 3e) and ubiquitination of HOIP was reduced significantly by Arginine (R) substitutions in K735, K783 and K875 (3×R; Supplementary Fig. 6c, lanes 4-6) and further by mutations of three adjacent residues K737, K784, and K873 (6×R; lanes 7-9). Finally, IpaH2.5 catalyzes K48-Ub conjugation of HOIP, which is recognized by the 26S proteasome subunit that mediates protein degradation (Fig. 3f)[29].

IpaH1.4/2.5 is the major E3 ligase regulator of cytokine RSCs

S. flexneri encodes 12 IpaH effector proteins including IpaH4.5, IpaH9.8 and IpaH0722 (IpaH5), which have been reported to target NF-κB subunit p65, NEMO and TRAF2, respectively, for degradation[13,15,30,31]. To directly test the contributions of chromosomal and plasmid encoded IpaH-type E3 ligases on innate immune evasion, a cellular degradation assay was performed with all major components of TNF and IL-1 RSCs. To first demonstrate the specificity of this assay, *Shigella* and *Salmonella* E3 ligases were expressed together with PKN1, a known *Salmonella* SspH1 substrate[28,32]. As expected, SspH1 induced the cellular degradation of PKN1, whereas other IpaH family members had no effect (Supplementary Fig. 8a, b). Contrary to previous studies[13,15,31], the reported targets of

IpaH4.5, IpaH9.8 and IpaH0722 (IpaH5) including p65, NEMO and TRAF2 were stable in the presence of *Shigella* IpaH proteins. In contrast, HOIP was readily degraded by IpaH1.4/2.5 (Fig. 4a). These results were confirmed by monitoring expression levels of endogenous HOIP, NEMO, p65 or TRAF2 in the presence of overexpressed *Shigella* IpaH proteins (Supplementary Fig. 9). We noted that during *Shigella* infection of CaCo-2 or U2OS cells only a fraction of cells were infected (Supplementary Fig. 3). Accordingly, HOIP levels were 53.8% (+/− 6.7) in *Shigella* infected CaCo-2 cells compared to uninfected control cells, while in the same samples endogenous NEMO was upregulated significantly and p65 or TRAF2 levels were not significantly altered (Fig. 4b). In addition, no other signaling components tested were degraded in the presence of IpaH proteins (Fig. 4 and Supplementary Fig. 9). These data reveal the central importance of IpaH1.4/2.5 among IpaH family members for blocking cytokine RSCs.

IpaH1.4 and OspI cooperate to limit RSC signaling during *Shigella* infection

Our studies now indicate that IpaH1.4/2.5 is a highly specific inhibitor of M1-Ub chain assembly. In addition, the *S. flexneri* M90T strain used in this study does not encode a functional OspZ[18], suggesting that OspI is the central effector targeting K63-Ub chains. Thus, we explored the question whether inhibition of M1- and K63-Ub chains by IpaH1.4/2.5 and OspI, respectively, are sufficient to suppress multiple RSCs during *Shigella* infection. To first determine if HOIP ubiquitination and degradation suppresses immune system activation during *Shigella* infection, we quantified endogenous NF-κB (p65) nuclear translocation at single cell resolution (Fig. 5a). Less than half (44.3+/−7.9%) of WT *Shigella* infected U2OS cells exhibited nuclear NF-κB accumulation (Fig. 5b). In contrast, NF-κB translocated to the nucleus in 94.3% (+/− 3.6) of U2OS cells infected with *ShigellaΔipaH1.4/2.5*, indicating that secretion of IpaH1.4/2.5 suppresses the host immune responses to PAMPs (Fig. 5a and b). Comparison between *ShigellaΔipaH1.4* and *ShigellaΔipaH2.5* mutant strains showed that IpaH1.4 is the essential T3SS effector protein required for blocking NF-κB activation (Fig. 5a and b), which is consistent with the role of IpaH1.4 in HOIP degradation during *Shigella* infection (Fig. 2e). Importantly, NF-κB activation by *ShigellaΔipaH1.4* was independent of the total bacterial load in infected cells and it was not due to alterations in bacterial intracellular growth characteristics (Fig. 5c and Supplementary Fig. 10). Interestingly, p65 readily accumulated in the nucleus of U2OS cells infected with *ShigellaΔospI* and *ShigellaΔipaH1.4ΔospI* strains indicating that similar to IpaH1.4, OspI secretion is required for immune suppression (Fig. 5a and b). These data indicate that IpaH1.4 and OspI perform non-redundant functions to inhibit PAMP-mediated NF-κB activation.

Cooperative termination of M1- and K63-Ub chain assembly limits the IL-1β response to pathogens

LUBAC post-translationally modifies numerous cytokine RSCs[2,3,33-36], suggesting that HOIP degradation may limit a broad spectrum of immune responses to *Shigella* infection. We found that WT *Shigella*, but not *ShigellaΔmxiD* (which lacks a functional T3SS), suppressed NF-κB nuclear translocation in response to IL-1β and TNF (Supplementary Fig. 11). In contrast, NF-κB accumulated in the nucleus of TNF and IL-1β stimulated U2OS and CaCo-2 cells infected with *Shigella* strains lacking either *ipaH1.4* or *ospI* genes, suggesting

that these effectors limit immune responses to these cytokines (Fig 6a, Supplementary Fig. 11, 12, 13). However, because NF-κB activation can occur by PAMPs under these conditions (see Figure 5a and b), we sought to more directly define the effects of M1- and K63-Ub chain elimination on cytokine signaling in genetically modified human cells.

We noted that cytokine RSCs exhibit different sensitivities to loss of M1-Ub chains as nuclear NF-κB was eliminated in TNF, but not IL-1β treated HOIP$^{-/-}$ cells (generated by CRIPSR/Cas9; Supplementary Fig. 14 and 15, Fig. 6b). Similar results were found in TAK1$^{-/-}$ cells that are unable to signal through K63-Ub chains (Fig. 6b and Supplementary Fig. 15). Thus, elimination of signaling through TNF-RSCs would require inhibition of either M1- or K63-Ub chain assembly, whereas IL-1β RSC inhibition would likely require loss of both.

To then deconstruct potential cooperative regulation of the IL-1β RSC by multiple T3SS effector proteins, we evaluated NF-κB nuclear translocation in HOIP$^{-/-}$ and TAK1$^{-/-}$ cells infected with *Shigella*. By genetically eliminating signaling through either M1-linked (HOIP$^{-/-}$) or K63-linked (TAK1$^{-/-}$) Ub chains allowed us to evaluate the relative contribution of IpaH1.4 and OspI on the IL-1β signaling pathway. As expected, similar to the WT *Shigella* strain, *ShigellaΔipaH1.4* suppressed IL-1β induced NF-κB nuclear translocation in HOIP$^{-/-}$ cells (which recapitulates HOIP degradation by IpaH1.4) (Fig. 6c). However, *ShigellaΔospI* or *ShigellaΔipaH1.4/ΔospI* strains lost this ability, confirming that in addition to elimination of linear polyubiquitin chains, inhibition of K63-linked polyubiquitin chain formation is required to suppress IL-1β signaling during infection. In TAK1$^{-/-}$ cells, which still generate K63-Ub chains but are unable to signal through these chains, the ability of *Shigella* to suppress IL-1β induced NF-κB translocation depended on both IpaH1.4 and OspI (Fig. 6d). The observed suppressive effect of OspI in TAK1$^{-/-}$ cells is likely due to the partial dependence of linear Ub chain generation on K63-linked Ub chains (Fig. 6e)[2,20]. Taken together, these data demonstrate that *Shigella* T3SS effector-mediated inhibitions of K63-linked and M1-linked ubiquitination is a critical step in suppressing signal transduction through diverse PRR and cytokine receptors (Fig. 6e).

Discussion

Here, we demonstrate that *Shigella flexneri* suppresses immune signal transduction by specifically recognizing the LUBAC machinery and targeting its enzymatic center HOIP for proteasomal degradation. In biochemical and cell based studies the *Shigella* E3 ubiquitin ligase IpaH1.4/2.5 directly interacted with LUBAC subunits HOIL-1L and HOIP, and catalyzed conjugation of K48-linked Ub chains to the RBR domain of HOIP. Proteasome dependent degradation of HOIP by IpaH1.4/2.5 was required for suppression of immune receptor signaling in NF-κB-luciferase assays as well as during *Shigella* infection. *S. flexneri* effectors that target components of innate immune RSCs have been reported previously[13,15,17,18,31]. However, except for OspI and OspZ we have not been able to reproduce these results. Unexpectedly, we found that the effectors IpaH4.5, IpaH9.8 and IpaH0722 had no effect on cytokine RSC signaling as suggested by previous reports[13,15,31]. These findings were confirmed in NF-κB activation assays (Figure 1, Supplementary Figure 1), in proteasomal degradation studies (Figure 4a, Supplementary Figure 9), and by bacterial

infection of model intestinal epithelial cells (Figure 4b). In contrast, we found that the cooperative functions of IpaH1.4 and OspI (by elimination of linear and K63-linked ubiquitination) were necessary to suppress NF-κB activation in response to IL-1β, TNF and bacterial PAMPs.

Linear ubiquitination has been associated with signaling through broad subsets of cytokine receptors (e.g. TNF-R1, IL-1R) and PRRs (e.g. NOD2, TLR4 and NLRP3)[2,20,33-36]. In fact, human patients with loss of function mutations in human HOIL-1L and HOIP genes are severely immunocompromised and especially susceptible to pyogenic bacterial infections[8,9]. Thus, the ability to deactivate LUBAC, may increase virulence of invasive enteric pathogens such as *Shigella* spp. in immunocompetent patients. *Shigella* spp. are transmitted via the feco-oral route and invade the colonic and rectal mucosa of humans. Although infection with *Shigella* leads to severe inflammation and mucosal destruction during late stages of infection[37,38], it is possible that LUBAC inactivation and suppression of NF-κB activation is important during early stages of *Shigella* invasion and infection of intestinal epithelial cells[39,40]. Taken together, these findings increase our understanding of how bacterial pathogens target innate immune signaling pathways and open up new ways to probe complex immune pathologies caused by LUBAC dysfunction.

Methods

NF-κB luciferase reporter assay

Shigella flexneri M90T genes encoding OspI, OspG, IpaH1.4, IpaH2.5, IpaH9.8 and *Shigella dysenteriae* gene encoding OspZ were PCR amplified and cloned into pEGFP-C2. pFlagCMV6b plasmids carrying Flag-TRAF2, Flag-Tab2, Flag-Tab3 or Flag-HOIL-1L and pcDNA3.1 plasmids carrying Myc-HOIP or Flag-His_6-SHARPIN were transfected, in indicated combinations, into HEK293T cells in a 48 well (10,000 cells/well) for 48h. The cells were co-transfected with plasmids carrying NF-κB-luc (pNF-κB) and lacZ (pLacZ, to correct for transfection efficiency using a beta-galactosidase assay) and with GFP-effector (pEGFP-C2) plasmids. After 48h cells were lysed and luciferase was measured according to manufacturer protocol (Promega).

Yeast 2-Hybrid assay

Shigella flexneri M90T genes encoding OspG, IpaH2.5 and IpaH4.5 were cloned into vector pLexNA. After introduction of constructed plasmids into *Saccharomyces cerevisiae* L40, expression of OspG, IpaH2.5 and IpaH4.5 was confirmed by Western blotting using anti-LexA antibodies (Millipore). In this Y2H screen LexA-effector expressed in the yeast *Saccharomyces cerevisiae* L40 served as the bait and a library of mouse embryo cDNA cloned in the vector pVP16 served as the prey as previously described[41,42]. The pLexNA plasmid provides L40 the ability to grow on Trp^- minimal medium (SD –W), and the pVP16 plasmid on Leu^- (SD –L) medium. An interaction between bait and prey allows LexA to be shuttled into the nucleus (via the NLS of VP16) resulting in expression of LacZ and HIS3 genes, and growth in Trp^-, Leu^-, His^- (SD –WHULK) medium. Plasmids were isolated from yeast colonies growing on SD – WHULK (+ 3 mM 3-Amino-1,2,4-triazole) using phenol/chloroform and were electroporated into *E. coli* HB101 strain. The pVP16 and

pLexNA plasmids were isolated from *E. coli* and inserts in pVP16 were sequenced using the pVP16 5' primer. For hits, pVP16 plasmids were isolated and reintroduced together with pLexNA plasmids containing effectors into the L40 yeast strain. Drops of tenfold dilution of colonies picked from SD –UWL plates were plated on SD –UWL and SD –WHULK plates.

GST pulldowns

$HOIP_{UBA-RBR}$ fragment was fused to the C-terminus of GST (in pGEX6P-1) and GST purified using glutathione coated beads. IpaH2.5 full length was fused to the C-terminus of His_6-MBP-His_6 (in pET28b) and His-tag purified on Ni-NTA beads. GST beads were loaded with 20 ug GST or GST-$HOIP_{UBA-RBR}$ for 2h, washed 3x and then incubated for 2h with His_6-MBP-HOIL-$1L_{UBL}$ (1-137) followed by 2h incubation with His_6-MBP or His_6-MBP-IpaH2.5. Then beads were washed 6x, and proteins were eluted from the beads in 50 mM reduced glutathione, pH8.0 and run on a SDS-PAGE gel for Coomassie staining or Western blotting.

Immunoprecipitation (IP) assays

To test cellular interaction of HOIP with IpaH1.4/2.5, Cys to Ser mutations in IpaH proteins (IpaH1.4C368S, IpaH2.5C368S, IpaH4.5C379S, IpaH7.8C357S and IpaH9.8C337S) were generated by Quickchange mutagenesis (Stratagene). GFP-IpaHC/S proteins were co-expressed with Myc- or Flag-tagged HOIP in 293T cells. 38 h after transfection cells were collected, washed once in cold PBS and lysed in buffer containing 25 mM Tris-HCl (pH7.4), 150 mM NaCl, 1% Triton, 1x protease inhibitor (Sigma Aldrich). Lysate was first pre-cleared with 15 µl ProteinA agarose beads (Thermo Scientific) for 1h. To IP Myc-HOIP or Flag-HOIP 2 µg anti-Myc (Covance) or anti-Flag (Sigma Aldrich) antibody was added for 1h followed by addition of 15 µl Protein-A agarose beads for 1.5h. Beads were then washed 10 times in lysis buffer and 50 µl 2x SDS loading buffer (Biorad) was added. For mapping experiments IP was performed using 2 µg anti-GFP antibodies (Clontech).

Cellular Degradation Assays

To determine IpaH1.4/2.5 mediated degradation of HOIP as part of LUBAC I, II or III, HEK293T cells (seeded in 6 well at 2.5×10^5 cells/well) were transfected with (0.35 µg/well) pEGFP-C2 plasmids carrying *ipaH* genes together with (0.15 µg/well) pFlagCMV6b-HOIL-1L, (0.15 µg/well) pcDNA3.1-Flag-His_6-SHARPIN and (0.7 µg/well) pcDNA3.1-Myc-HOIP using Fugene HD at 3:1 ratio (µl Fugene HD: µg total DNA). After 24h cells were lysed in 100 µl buffer containing 25 mM Tris-HCl (pH7.4), 150 mM NaCl, 1% Triton and 1x protease inhibitor (Sigma Aldrich) and added to equal volume of 2x SDS loading buffer (Biorad) for SDS-PAGE and Western blotting. For degradation assays with HOIP fragments, pcDNA3.1-Flag-His_6 plasmids carrying HOIP fragments, were co-transfected with pEGFP-C2-IpaH2.5 (WT or C368S), following above described method.

For proteasome inhibition experiments HEK293T cells (seeded in 6 well at 2.5×10^5/well) were transfected with pcDNA3.1-Flag-HOIP, pFlagCMV6b-HOIL-1 and pEGFP-C2-IpaH1.4 or IpaH2.5 (WT or C368S) for 16h (overnight) and then treated with either 10µM MG132 (Sigma Aldrich) or with an equal volume of vehicle (DMSO) as control for 24h.

Then cells were collected in 120 μl 2x SDS loading buffer (Biorad) per well followed by SDS-PAGE and Western blotting.

To screen for cytokine RSC targets for *Shigella* IpaH proteins, HEK293T cells (seeded 8h earlier into 12 well plates at 1×10^5 cells/well) were transfected with pEGFP-C2 plasmids carrying *ipaH* genes (0.35 μg/well) together with pFlagCMV6b plasmids carrying human genes encoding immune signaling components (0.15 μg/well), using Fugene HD (Promega) at 3:1 ratio (μl Fugene HD: μg total DNA). After 40h cells were collected in 60 μl 2x SDS loading buffer (Biorad) per well followed by SDS-PAGE and Western blotting.

Genes encoding IpaH1.4, IpaH2.5, IpaH4.5, IpaH7.8 and IpaH9.8 were amplified from *Shigella flexneri* M90T virulence plasmid, and genes encoding IpaH proteins located on the chromosome (described in ref [30]): IpaH1/IpaH6 = IpaH2610/IpaH0887 (*Shigella flexneri* M90T ORF SF5M90T_2545/SF5M90T_744), IpaH2 = IpaH1880 (SF5M90T_1825), IpaH3 = IpaH1383 (SF5M90T_1355), IpaH4/IpaH7 = IpaH2022/IpaH2202 (SF5M90T_1966/ SF5M90T_2130) and IpaH5 = IpaH0722 (SF5M90T_2665) were amplified from *Shigella flexneri* M90T chromosomal DNA. Genes encoding *Salmonella* SspH1, SspH2 and SlrP proteins were amplified from *S. enterica* Typhimurium LT2 chomosomal DNA. E3 ligase effector genes were cloned into pEGFP-C2 using Gibson cloning method (New England Biolabs). Human genes encoding signaling components were amplified from Ultimate human ORF collection (Thermo Fisher Scientific) and cloned into pFlagCMV-6b plasmids using Gibson cloning method (New England Biolabs).

In vitro Ubiquitination assays

Shigella flexneri genes encoding IpaH proteins were cloned into pGEX4T-1, expressed in *E. coli* BL21 and purified using glutathione coated beads. His_6-UbcH5b and His_6-UbE1 were expressed in *E. coli* BL21 and purified using Ni-NTA agarose beads (Qiagen). LUBAC (Flag-HOIL-1L/Myc-HOIP/Flag-His_6-SHARPIN) was expressed in HeLa cells and purified using Ni-NTA agarose beads (Qiagen). LUBAC purified from HeLa cells was then used in an Ub reaction, containing 0.1 μM UbE1 (E1), 2.5 μM UbcH5b (E2), 5 μM (Flag, HA or His_6 tagged) Ub (BostonBiochem), 0.5 mM $MgSO_4$, 0.5 mM ATP, 20 units/ml inorganic pyrophosphatase (Sigma Aldrich), 1 mM DTT and 50 nM GST-IpaH (E3). After 0, 20, 60 or 90 minutes incubation at 37°C samples were electrophoresed on an SDS PAGE buffer and a Western blot was stained with anti-Myc antibodies. Wild type Ub (Flag, HA, His_6 tagged), K48 only Ub (His_6 tagged) and K48R (His_6 tagged) were purchased from BostonBiochem.

Mass Spectrometry

To determine which lysines in HOIP are ubiquitinated by IpaH2.5, an Ub reaction (500 μl volume) was performed with GST-IpaH2.5 or GST-IpaH2.5C368S, and after 90 mins at 37°C, Myc-HOIP was immunoprecipitated (IP) using anti-Myc antibodies (Covance). The IP fractions were then run on a SDS-PAGE gel (Biorad) and Coomassie stained bands were excised and proteins were digested in-gel with trypsin and run on a Q Exactive MS platform at the Mass Spectrometry Core at UTSW.

Infections of tissue culture cells and microscopy

For infections with *Shigella flexneri* M90T, strains were grown overnight at 30°C in Brain Heart Infusion (BHI) broth (BD Biosciences) followed by 1:50 dilution in BHI broth and additional 2h growth at 37°C to an OD_{600nm} of 0.4 to 0.6. Bacteria were then washed 1x in PBS and resuspended in 0.03% Congo Red (Sigma Aldrich) for 15 min at 37°C prior to infection of cells. *Listeria monocytogenes* were grown overnight at 30°C in BHI broth prior to infection of cells. After addition (at indicated MOI) of *Shigella* or *Listeria* strains to HeLa, U2OS or CaCo-2 cells (grown in DMEM + 10% FBS), infection was initiated through centrifugation of plates at 1000g for 10 mins, followed by incubation at 37°C, 5% CO_2, for 90 mins. To kill extracellular bacteria, media was then replaced with DMEM + 50 μg/ml gentamycin. After indicated time points samples were then processed. For CFU enumeration, cells were washed 2x with PBS, lysed in 1% Triton-X100 in PBS, and serial dilutions were plated on LB plates. For Western Blotting cells were washed once in PBS and lysed in 2x SDS loading buffer. For p65 translocation immunofluorescence experiments, cells on coverslips were washed 2x in PBS, fixed in 10% formaldehyde for 10 mins, washed 2x in PBS, permeabilized (in 10% Horse serum, 0.5% Triton X100, PBS) for 45 mins, stained for 10 mins in primary antibody (anti-p65 from Cell Signalling in 10% Horse serum, 0.5% Triton X100, PBS) for 45 mins, washed 3x in PBS, stained with secondary antibody (Fluorescein conjugated goat anti-rabbit from Pierce in 10% Horse serum, 0.5% Triton X100, PBS + DAPI and Alexa Fluor 594 Phalloidin from Life Sciences), washed 3x in PBS and 1x in H_2O followed by mounting of the coverslips on glass slides. A Zeiss Observer Z1 fluorescent microscope and Zeiss software Zen were used to obtain and process images. At least 10 images/slide were obtained each experiment. Quantification of translocation of p65 to the nucleus was manually scored. In uninfected samples (and infections with *Shigella ΔmxiD*) all cells were included, while in infected samples only infected cells (based on the presence of DAPI stained bacteria in the cytoplasm of cells) were included. A p65 signal lower in the nucleus compared to cytoplasm was scored as no translocation and a p65 signal higher in the nucleus compared to cytoplasm was scored as translocation. The outline of cells in a monolayer was determined by visualizing the cytoskeleton of cells using Phalloidin stain. Fluorescence intensity in cross sections of cells was determined using the plot profile tool in Image J.

Reagents

Antibodies used are anti-LexA (06-719, Millipore), anti-Myc 9E10 (MMS-150P, Covance), anti-Flag M2 (A8592, Sigma Aldrich), anti-GFP (632592, Clontech), anti-Actin (A2066, Sigma Aldrich), anti-HOIP (MAB8039, R&D systems), anti-RBCK1/HOIL-1L (HPA024185, Sigma Aldrich). Anti-Phospho-IκBα (2859), anti-IκBα (4814), anti-Phospho-p65 (3033), anti-p65 (8242), anti-TRADD (3684), anti-TRAF2 (4712), anti-IKKα (11930), anti-TNF-R1 (3736) and anti-TAK1 (4505) were purchased from Cell Signaling. Anti-IKBKG/NEMO antibodies were purchased from Sigma Aldrich (SAB1404591) and Millipore (05-631).

Cell lines used in this study HEK293T (CRL-3216), HeLa (CCL-2), CaCo-2 (HTB-37) and U2OS (HTB-96) were purchased from ATCC. Parental cell lines were tested and determined to be mycoplasma free.

Statistical analysis

A two-tailed unpaired Student's *t*-test was used to calculate statistical differences. Experiments were performed at least three times independently. A *P*-value of less than 0.05 was considered significant.

Construction of *Shigella* mutants

A *Shigella flexneri* M90T Δ*ipaH1.4,* Δ*ipaH2.5 and* Δ*ospI* single and double mutants were constructed by λ red recombinase mediated replacement by homologous recombination of respective genes with a kanamycin resistance cassette followed by FLP recombinase catalyzed removal of the cassette[43]. Primers used were *ipaH1.4-F* (CGGTTCTGGCATTATGCATCAAATAAACAATGTATACTCGTTAACTCCATTAGTGTAGGCTGGAGCTGCTTC) and *ipaH1.4-R* (TCCCATAGAGAAAAATATTCGAGGACCAGAATAATCTGGTCCGGTGGTTACAGCCATATGAATATCCTCCTTAG) for deletion of *ipaH1.4.* For deletion of *ipaH2.5* primers *ipaH2.5-F* (GATTAAATCAACAAATATACAGGTAATCGGTTCTGGTATTATGCATCAAAGTGTAGGCTGGAGCTGCTTC) and *ipaH2.5-R* (GTGTTCTGGAGCGGAAATTGTGGCAGAATTTCCCATAGAGAAAAATATTCGCAGCCATATGAATATCCTCCTTAG) were used. For the Δ*ipaH1.4/2.5* double mutant this procedure was repeated for the *ipaH1.4* gene in Δ*ipaH2.5* background using primers *ipaH1.4-F2* (GATTAAATCAACCAATATACAGGCAATCGGTTCTGGCATTATGCATCAAAGTGTAGGCTGGAGCTGCTTC) and *ipaH1.4-R2* (GGCCAGTACCTCGTCAGTCAACTGACGGTAAATCTGCTGTTCAGTCTCACGCCAGCCATATGAATATCCTCCTTAG). To make Δ*ospI* single mutant or Δ*ospI* in Δ*ipaH1.4* background (Δ*ipaH1.4*/Δ*ospI*) primers *ospI-F* (GGTGTCGTTACAGGGAACTGCTGGATATGAGGCACATACAGAGGAGGGAAATGTGTAGGCTGGAGCTGCTTC) and *ospI-R* (CAGCAAAGCCTCTTACTTTTCCAACTACTACTGTTAGCATAGTGATCAAATTCCAGCCATATGAATATCCTCCTTAG) were used.

Briefly, a kanamycin resistance cassette (matching primer sequences are underlined) flanked with ~50 base pairs homologous to the gene of interest was amplified from plasmid DNA (pKD3). PCR products were electroporated into *Shigella flexneri* strain M90T carrying the red recombinase plasmid pKD46. Transformants were selected by growth on LB agar plates containing kanamycin (50μg/ml) and simultaneously cured of pKD46 by growth at 42°C overnight. The kanamycin resistance gene was eliminated through the introduction of the pCP20 helper plasmid that contains the FLP recombinase. Subsequent curing of pCP20 was carried out by growing strains at 42°C for 5 hours. Deletions were confirmed by PCR using primers flanking the deletion site, and sequencing of the PCR product.

Construction *Listeria monocytogenes* strains

Shigella effectors IpaH2.5 (wt and C368S) were cloned into pActAN100-pPL2[44], in which effectors were Gibson assembled (New England Biolabs) together with a 3×Flag-tag and a

529 nt *Listeria monocytogenes actA* fragment (247 nt of the *actA* promoter region and 282 nt of the *actA* ORF). Thus, the resulting construct ActA(1-94aa)-3×Flag-IpaH2.5(aa 1-563) contains the ActA Sec secretion signal from *Listeria* and is under transcriptional control of the *actA* promoter. The resulting plasmids were introduced into the (attenuated) *Listeria* 10403S Δ*inlA* strain through conjugation with *E. coli* SM10.

CRISPR/Cas9 genome editing

For CRISPR/Cas9 mediated knockout of MAP3K7/TAK1 or RNF31/HOIP from U2OS cells a previously described method was used [45,46]. The sequences TTGTCCGCTGCAACGCTCAT in the first exon of RNF31 gene and GATCGACTACAAGGAGATCG in the first exon of MAP3K7 gene were cloned into lentiCRISPRv2 vector, and introduced into U2OS cells through Lentiviral infection, to facilitate genomic targeting of these sites by Cas9. After obtaining a culture derived from a single cell, knockout of RNF31/HOIP or MAP3K7/TAK1 was confirmed by Western blotting and sequencing of the affected site.

Supplementary Material

Refer to Web version on PubMed Central for supplementary material.

Acknowledgements

The authors would like to thank K. Iwai (Kyoto University) and T. Sixma (The Netherlands Cancer Institute) for providing plasmids, R. Potts (UTSW) for reagents and advice, and the Alto lab for helpful discussions. We acknowledge the services of the University of Texas Southwestern Medical Center proteomics core. The authors have no conflict of interest. This work was supported by grants from the National Institute of Health (AI083359 and GM100486), the Welch Foundation (#I-1704), and the Burroughs Wellcome Fund to N.M.A.

References

1. Gerlach B, et al. Linear ubiquitination prevents inflammation and regulates immune signalling. Nature. 2011; 471:591–596. doi:10.1038/nature09816. [PubMed: 21455173]
2. Haas TL, et al. Recruitment of the linear ubiquitin chain assembly complex stabilizes the TNF R1 signaling complex and is required for TNF-mediated gene induction. Molecular cell. 2009; 36:831–844. doi:10.1016/j.molcel.2009.10.013. [PubMed: 20005846]
3. Ikeda F, et al. SHARPIN forms a linear ubiquitin ligase complex regulating NF-kappaB activity and apoptosis. Nature. 2011; 471:637–641. doi:10.1038/nature09814.
4. Walczak H, Iwai K, Dikic I. Generation and physiological roles of linear ubiquitin chains. BMC biology. 2012; 10:23. doi:10.1186/1741-7007-10-23.
5. Rieser E, Cordier SM, Walczak H. Linear ubiquitination: a newly discovered regulator of cell signalling. Trends in biochemical sciences. 2013; 38:94–102. doi:10.1016/j.tibs.2012.11.007. [PubMed: 23333406]
6. Rahighi S, et al. Specific recognition of linear ubiquitin chains by NEMO is important for NF-kappaB activation. Cell. 2009; 136:1098–1109. doi:10.1016/j.cell.2009.03.007. [PubMed: 19303852]
7. Tokunaga F, et al. Involvement of linear polyubiquitylation of NEMO in NF-kappaB activation. Nature cell biology. 2009; 11:123–132. doi:10.1038/ncb1821. [PubMed: 19136968]
8. Boisson B, et al. Human HOIP and LUBAC deficiency underlies autoinflammation, immunodeficiency, amylopectinosis, and lymphangiectasia. The Journal of experimental medicine. 2015 doi:10.1084/jem.20141130.

9. Boisson B, et al. Immunodeficiency, autoinflammation and amylopectinosis in humans with inherited HOIL-1 and LUBAC deficiency. Nature immunology. 2012; 13:1178–1186. doi:10.1038/ni.2457. [PubMed: 23104095]
10. Reddick LE, Alto NM. Bacteria fighting back: how pathogens target and subvert the host innate immune system. Molecular cell. 2014; 54:321–328. doi:10.1016/j.molcel.2014.03.010. [PubMed: 24766896]
11. Kotloff KL, et al. Global burden of Shigella infections: implications for vaccine development and implementation of control strategies. Bulletin of the World Health Organization. 1999; 77:651–666. [PubMed: 10516787]
12. Lan R, Alles MC, Donohoe K, Martinez MB, Reeves PR. Molecular evolutionary relationships of enteroinvasive Escherichia coli and Shigella spp. Infection and immunity. 2004; 72:5080–5088. doi:10.1128/IAI.72.9.5080-5088.2004. [PubMed: 15322001]
13. Ashida H, et al. A bacterial E3 ubiquitin ligase IpaH9.8 targets NEMO/IKKgamma to dampen the host NF-kappaB-mediated inflammatory response. Nature cell biology. 2010; 12:66–73. sup pp 61-69. doi:10.1038/ncb2006. [PubMed: 20010814]
14. Buchrieser C, et al. The virulence plasmid pWR100 and the repertoire of proteins secreted by the type III secretion apparatus of Shigella flexneri. Molecular microbiology. 2000; 38:760–771. [PubMed: 11115111]
15. Ashida H, Nakano H, Sasakawa C. Shigella IpaH0722 E3 ubiquitin ligase effector targets TRAF2 to inhibit PKC-NF-kappaB activity in invaded epithelial cells. PLoS pathogens. 2013; 9:e1003409. doi:10.1371/journal.ppat.1003409. [PubMed: 23754945]
16. Kim DW, et al. The Shigella flexneri effector OspG interferes with innate immune responses by targeting ubiquitin-conjugating enzymes. Proceedings of the National Academy of Sciences of the United States of America. 2005; 102:14046–14051. doi:10.1073/pnas.0504466102. [PubMed: 16162672]
17. Sanada T, et al. The Shigella flexneri effector OspI deamidates UBC13 to dampen the inflammatory response. Nature. 2012; 483:623–626. doi:10.1038/nature10894. [PubMed: 22407319]
18. Newton HJ, et al. The type III effectors NleE and NleB from enteropathogenic E. coli and OspZ from Shigella block nuclear translocation of NF-kappaB p65. PLoS pathogens. 2010; 6:e1000898. doi:10.1371/journal.ppat.1000898. [PubMed: 20485572]
19. Zhang L, et al. Cysteine methylation disrupts ubiquitin-chain sensing in NF-kappaB activation. Nature. 2012; 481:204–208. doi:10.1038/nature10690. [PubMed: 22158122]
20. Emmerich CH, et al. Activation of the canonical IKK complex by K63/M1-linked hybrid ubiquitin chains. Proceedings of the National Academy of Sciences of the United States of America. 2013; 110:15247–15252. doi:10.1073/pnas.1314715110. [PubMed: 23986494]
21. Rohde JR, Breitkreutz A, Chenal A, Sansonetti PJ, Parsot C. Type III secretion effectors of the IpaH family are E3 ubiquitin ligases. Cell host & microbe. 2007; 1:77–83. doi:10.1016/j.chom.2007.02.002. [PubMed: 18005683]
22. Zhu Y, et al. Structure of a Shigella effector reveals a new class of ubiquitin ligases. Nature structural & molecular biology. 2008; 15:1302–1308. doi:10.1038/nsmb.1517.
23. Pruneda JN, et al. E2~Ub conjugates regulate the kinase activity of Shigella effector OspG during pathogenesis. The EMBO journal. 2014; 33:437–449. doi:10.1002/embj.201386386. [PubMed: 24446487]
24. Zhou Y, Dong N, Hu L, Shao F. The Shigella type three secretion system effector OspG directly and specifically binds to host ubiquitin for activation. PloS one. 2013; 8:e57558. doi:10.1371/journal.pone.0057558. [PubMed: 23469023]
25. Uekusa Y, et al. Backbone and side chain 1H, 13C, and 15N assignments of the ubiquitin-like domain of human HOIL-1L, an essential component of linear ubiquitin chain assembly complex. Biomolecular NMR assignments. 2012; 6:177–180. doi:10.1007/s12104-011-9350-1. [PubMed: 22127525]
26. Yagi H, et al. A non-canonical UBA-UBL interaction forms the linear-ubiquitin-chain assembly complex. EMBO reports. 2012; 13:462–468. doi:10.1038/embor.2012.24. [PubMed: 22430200]

27. Smit JJ, et al. The E3 ligase HOIP specifies linear ubiquitin chain assembly through its RING-IBR-RING domain and the unique LDD extension. The EMBO journal. 2012; 31:3833–3844. doi: 10.1038/emboj.2012.217. [PubMed: 22863777]
28. Keszei AF, et al. Structure of an SspH1-PKN1 complex reveals the basis for host substrate recognition and mechanism of activation for a bacterial E3 ubiquitin ligase. Molecular and cellular biology. 2014; 34:362–373. doi:10.1128/MCB.01360-13. [PubMed: 24248594]
29. Chau V, et al. A multiubiquitin chain is confined to specific lysine in a targeted short-lived protein. Science. 1989; 243:1576–1583. [PubMed: 2538923]
30. Ashida H, Toyotome T, Nagai T, Sasakawa C. Shigella chromosomal IpaH proteins are secreted via the type III secretion system and act as effectors. Molecular microbiology. 2007; 63:680–693. doi: 10.1111/j.1365-2958.2006.05547.x. [PubMed: 17214743]
31. Wang F, et al. Shigella flexneri T3SS effector IpaH4.5 modulates the host inflammatory response via interaction with NF-kappaB p65 protein. Cellular microbiology. 2013; 15:474–485. doi: 10.1111/cmi.12052. [PubMed: 23083102]
32. Haraga A, Miller SI. A Salmonella type III secretion effector interacts with the mammalian serine/threonine protein kinase PKN1. Cellular microbiology. 2006; 8:837–846. doi:10.1111/j.1462-5822.2005.00670.x.
33. Damgaard RB, et al. The ubiquitin ligase XIAP recruits LUBAC for NOD2 signaling in inflammation and innate immunity. Molecular cell. 2012; 46:746–758. doi:10.1016/j.molcel.2012.04.014. [PubMed: 22607974]
34. Gurung P, Lamkanfi M, Kanneganti TD. Cutting edge: SHARPIN is required for optimal NLRP3 inflammasome activation. Journal of immunology. 2015; 194:2064–2067. doi:10.4049/jimmunol.1402951.
35. Rodgers MA, et al. The linear ubiquitin assembly complex (LUBAC) is essential for NLRP3 inflammasome activation. The Journal of experimental medicine. 2014; 211:1333–1347. doi: 10.1084/jem.20132486. [PubMed: 24958845]
36. Tokunaga F, et al. SHARPIN is a component of the NF-kappaB-activating linear ubiquitin chain assembly complex. Nature. 2011; 471:633–636. doi:10.1038/nature09815. [PubMed: 21455180]
37. Raqib R, Wretlind B, Andersson J, Lindberg AA. Cytokine secretion in acute shigellosis is correlated to disease activity and directed more to stool than to plasma. The Journal of infectious diseases. 1995; 171:376–384. [PubMed: 7531208]
38. Speelman P, Kabir I, Islam M. Distribution and spread of colonic lesions in shigellosis: a colonoscopic study. The Journal of infectious diseases. 1984; 150:899–903.
39. Islam D, et al. Downregulation of bactericidal peptides in enteric infections: a novel immune escape mechanism with bacterial DNA as a potential regulator. Nature medicine. 2001; 7:180–185. doi:10.1038/84627.
40. Sperandio B, et al. Virulent Shigella flexneri subverts the host innate immune response through manipulation of antimicrobial peptide gene expression. The Journal of experimental medicine. 2008; 205:1121–1132. doi:10.1084/jem.20071698. [PubMed: 18426984]
41. Fields S, Song O. A novel genetic system to detect protein-protein interactions. Nature. 1989; 340:245–246. doi:10.1038/340245a0. [PubMed: 2547163]
42. Hollenberg SM, Sternglanz R, Cheng PF, Weintraub H. Identification of a new family of tissue-specific basic helix-loop-helix proteins with a two-hybrid system. Molecular and cellular biology. 1995; 15:3813–3822. [PubMed: 7791788]
43. Datsenko KA, Wanner BL. One-step inactivation of chromosomal genes in Escherichia coli K-12 using PCR products. Proceedings of the National Academy of Sciences of the United States of America. 2000; 97:6640–6645. doi:10.1073/pnas.120163297. [PubMed: 10829079]
44. Lauer P, Chow MY, Loessner MJ, Portnoy DA, Calendar R. Construction, characterization, and use of two Listeria monocytogenes site-specific phage integration vectors. Journal of bacteriology. 2002; 184:4177–4186. [PubMed: 12107135]
45. Sanjana NE, Shalem O, Zhang F. Improved vectors and genome-wide libraries for CRISPR screening. Nature methods. 2014; 11:783–784. doi:10.1038/nmeth.3047. [PubMed: 25075903]
46. Shalem O, et al. Genome-scale CRISPR-Cas9 knockout screening in human cells. Science. 2014; 343:84–87. doi:10.1126/science.1247005. [PubMed: 24336571]

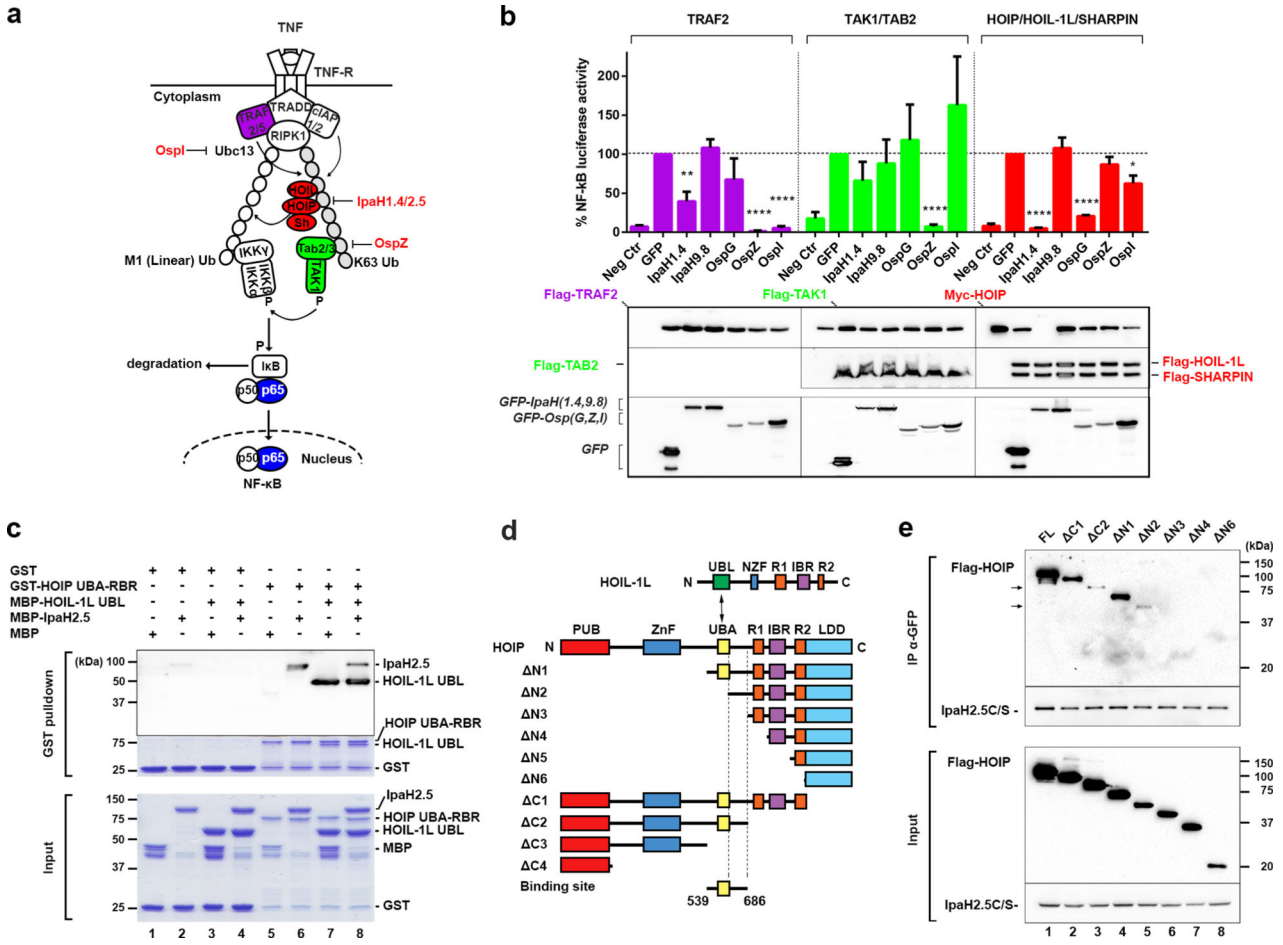

Figure 1. Screening *Shigella flexneri* T3SS effector proteins for disrupting the TNF-R signaling pathway

a, Schematic of the TNF-R signaling complex leading to NF-κB translocation to the nucleus. Components of the pathway expressed in HEK293T cells (in **b**) are colored. **b,** NF-κB activation by cellular expression of components of the TNF-RSC is inhibited by *Shigella* effectors as measured using a NF-κB luciferase assay. *P<0.05, **P<0.01, ****P<0.0001 (unpaired two-tailed t-test compared to GFP control). Data are presented as the mean +/− s.d. of three independent experiments. Western blots show expression of Flag- or Myc-tagged TNF-RSC components and GFP-tagged effector proteins. **c,** GST pulldown shows that MBP-His_6-IpaH2.5 interacts with mini-LUBAC (GST-$HOIP_{UBA-RBR}$, residues 557-1072, in complex with MBP-His_6-$HOIL\text{-}1L_{UBL}$, residues 1-134). Top panel is Western blot probed with anti-His antibodies. Second panel from the top shows same pulldown samples in Coomassie stained SDS-PAGE gel. Bottom panel shows input samples in Coomassie stained SDS-PAGE gel. **d,** Schematic of Flag-HOIP fragments used in mapping assays. **e**, Immunoprecipitation using anti-GFP antibodies show that region upstream of RING1 in HOIP is required for interaction with GFP-$IpaH2.5_{C368S}$. Arrows indicate fragments interacting with low affinity (right panel). FL, full length. Results shown in **c** and **e** are representative of three independent experiments.

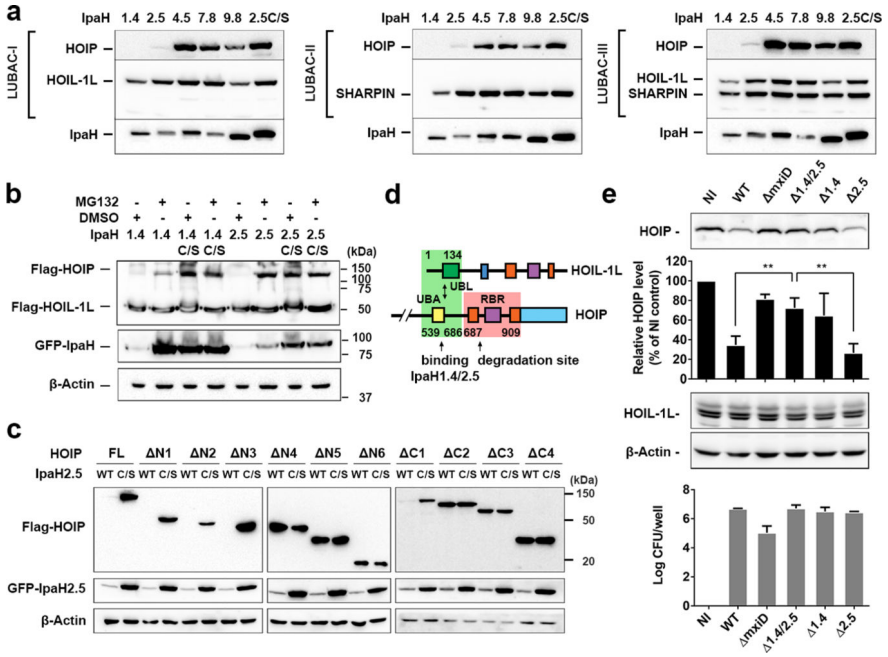

Figure 2. IpaH1.4/2.5 mediates proteasomal degradation of HOIP

a, HOIP, as part of LUBAC I, II or III (Myc-HOIP expressed together with Flag-HOIL-1L and/or Flag-His$_6$-SHARPIN), is absent in cells expressing GFP-IpaH1.4/2.5 as shown by Western blotting. **b,** Addition of 10μM MG132 protease inhibitor rescues Flag-HOIP protein stability in presence of GFP-IpaH1.4 or GFP-IpaH2.5. **c,** Mapping shows wild type GFP-IpaH2.5 (WT) but not GFP-IpaH2.5$_{C368S}$ (C/S) targets RING1 domain of Flag-HOIP for degradation. Results shown in **a-c** are representative of three independent experiments. **d**, Schematic of IpaH1.4/2.5 interaction and degradation sites in HOIP and HOIL-1L. **e**, Degradation of endogenous HOIP during infection with *S. flexneri* M90T depends on the *ipaH1.4* gene product. Western blots from three independent experiments were quantified and presented as the mean +/− s.d. **P<0.01 (unpaired two-tailed t-test). NI: not infected, WT: wild type *S. flexneri* M90T.

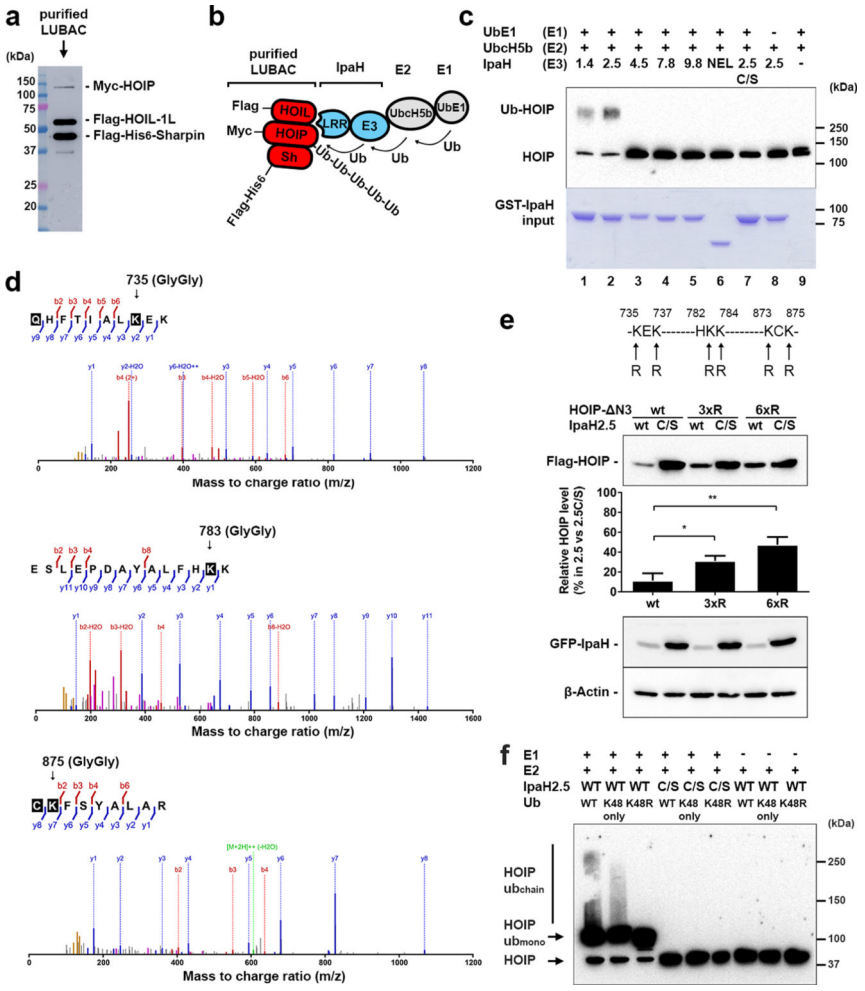

Figure 3. IpaH1.4/2.5 post-translationally modifies Lys residues 735, 783 and 875 in HOIP

a, LUBAC (Flag-His$_6$-SHARPIN, Myc-HOIP and Flag-HOIL-1L), was obtained from HeLa cell lysates by Ni-NTA affinity chromatography. Western blot shown was stained with anti-Myc followed by anti-Flag antibodies. **b,** Schematic of *in vitro* ubiquitination reaction in which purified LUBAC was mixed with recombinant human His$_6$-UbE1, His$_6$-UbcH5b, Flag-Ubiquitin, *Shigella* GST-IpaH and ATP. **c,** HOIP is specifically ubiquitinated in *in vitro* reactions by IpaH1.4/2.5. Top panel is a Western blot probed with anti-Myc antibodies. Second panel shows GST-IpaH input samples in Coomassie stained SDS-PAGE gel. **d,** Tandem mass (MS/MS) spectra of IpaH2.5 treated HOIP sample. High confidence assignment of ubiquitination on Lys 735, 783 and 875 was based on sequence coverage from y and b ions and miscleavage by trypsin due to GlyGly residues on Lys. In addition these lysines were not ubiquitinated in IpaH2.5$_{C368S}$ treated samples (see Supplementary Fig. 7). **e,** Lys to Arg mutations in residues 735, 783 and 875 (3×R) or 735, 737, 783, 784, 873, 875 (6×R) in Flag-His$_6$-HOIP fragment ΔN3 (aa 687-1072) reduces degradation by IpaH2.5. Western blots from three independent experiments were quantified. Data are presented as mean +/− s.d. *P<0.05, **P<0.01 (unpaired two-tailed t-test). **f,** IpaH2.5 can use wild type ubiquitin and K48-only ubiquitin (all Lys residues mutated to Arg except for Lys48), but not K48R ubiquitin (Lys48 mutated to Arg), to ligate ubiquitin chains (Ub$_{chain}$) to Flag-His$_6$-

HOIP fragment ΔN3. K48R ubiquitin can only be used for mono-ubiquitination (Ub_{mono}) of HOIP Lys residues by IpaH2.5. Results shown in **a**, **c**, **d** and **f** are representative of three independent experiments.

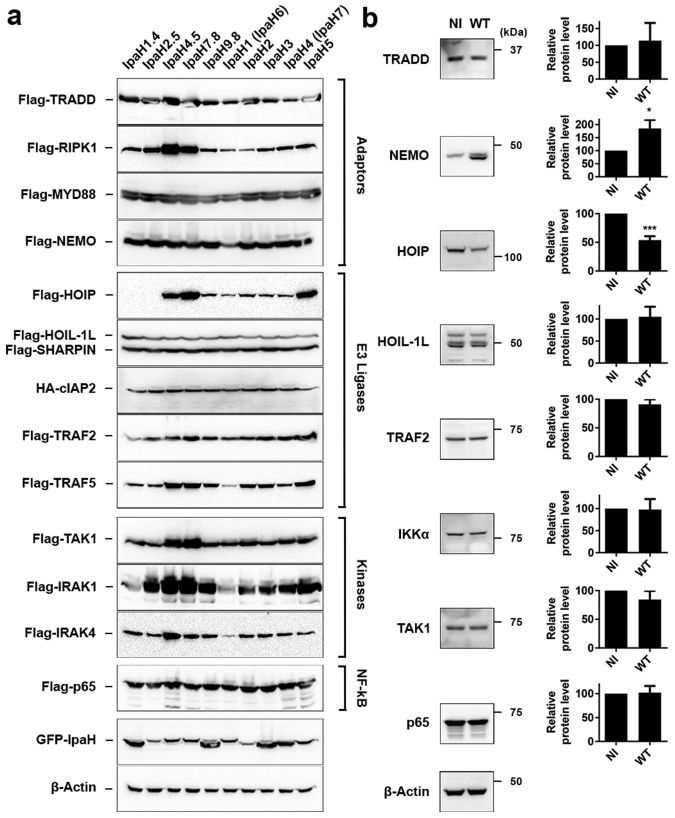

Figure 4. IpaH1.4 is the major E3 ligase regulator of cytokine RSCs

a, Degradation assay in HEK293T cells expressing GFP-tagged *Shigella* IpaH proteins in combination with TNF-R and IL-1R signaling components. Shown are representative Western blots from three independent experiments. *S. flexneri* IpaH6 and IpaH7 are nearly identical to IpaH1 and IpaH4, respectively[30]. IpaH1 is encoded by *S. fexneri* M90T ORF SF5M90T_2545, IpaH2 by SF5M90T_1825, IpaH3 by SF5M90T_1355, IpaH4 by SF5M90T_1966, IpaH5 by SF5M90T_2665, IpaH6 by SF5M90T_744 and IpaH7 by SF5M90T_2130. **b,** Western blotting shows that compared to non-infected control cells (NI), endogenous HOIP protein levels are reduced in CaCo-2 cells infected for 5h with *S. flexneri* M90T (WT) at MOI 150. No reduction in stability (in same samples) of endogenous TRAF2, NEMO, p65, HOIL-1L, TRADD, TAK1 or IKKα was detected. Western blots from three independent experiments were quantified and presented as the mean +/− s.d. *P<0.05, ***P<0,001, ns: not significant (unpaired two-tailed t-test).

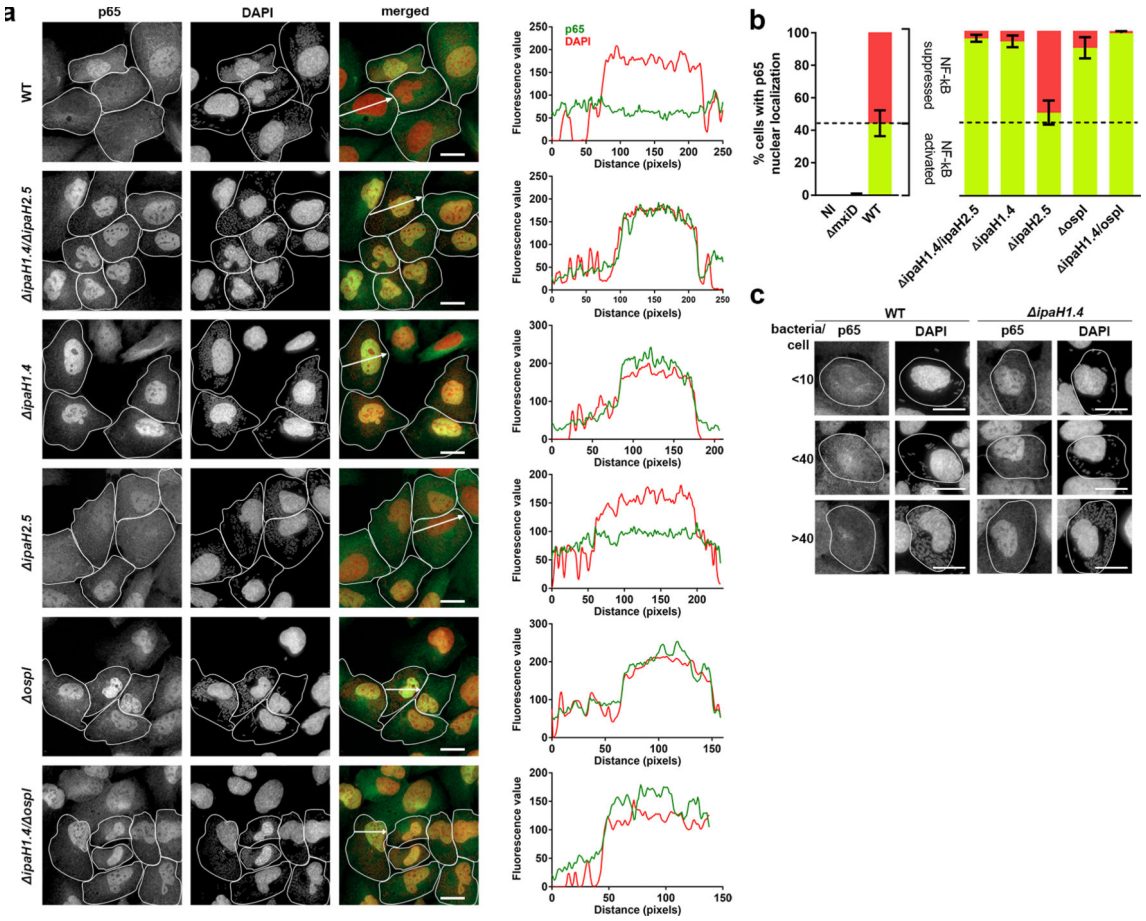

Figure 5. Innate immune pathways are disrupted by IpaH1.4 during infection

a, Representative fluorescent microscopy images of untreated wild type U2OS cells infected with *S. flexneri* strains are shown. Infected cells are outlined. Cells were stained with DAPI (pseudo colored red) to stain bacteria and nuclei of cells and anti-NF-κB subunit p65 antibodies (green). DAPI and p65 fluorescence intensity values in a cross section of a cell (indicated with a white arrow) are shown in graphs on the right. **b**, Nuclear translocation of p65 in U2OS cells was quantified as shown in bar graphs. *S. flexneri* M90T prevented nuclear translocation of p65 in infected cells and this depended on the presence of the *ipaH1.4* and *ospI* genes. Bar graphs represent results from three independent experiments presented as the mean +/− s.d. **c**, IpaH1.4 mediated suppression of p65 nuclear translocation by *S. flexneri* is independent of bacterial load. Images shown in **a** and **c** are representative results from three independent experiments. Scale bars, 20μm. NI, not infected.

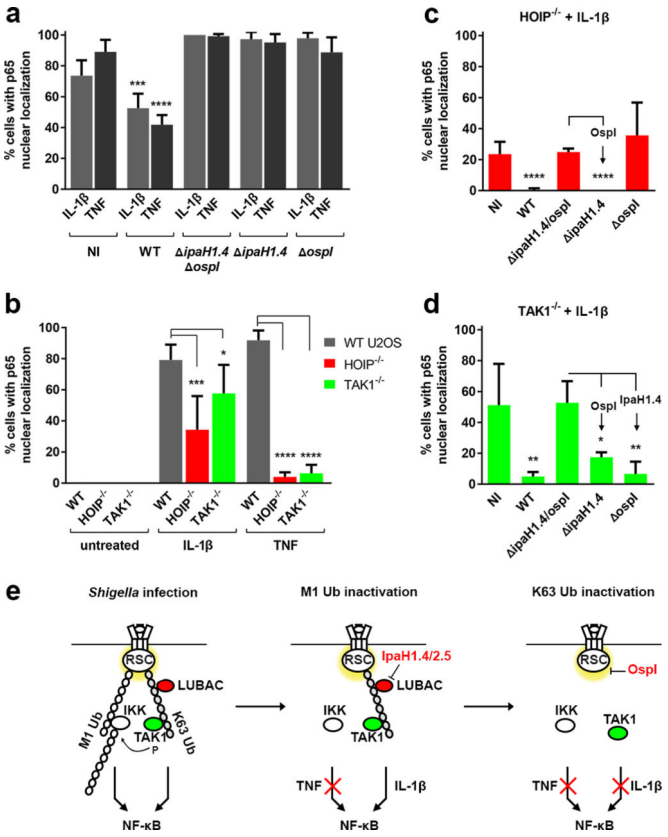

Figure 6. IpaH1.4 and OspI cooperate to limit IL-1R signaling during *Shigella* infection

a, *S. flexneri* M90T prevents nuclear translocation of p65 in infected cells, treated with 25 ng/ml IL-1β or TNF for 20 minutes and this depends on the presence of the *ipaH1.4* and *ospI* genes. NI, not infected. **b,** Quantification of p65 translocation to the nucleus in wild type, RNF31 (HOIP)$^{-/-}$ and MAP3K7 (TAK1)$^{-/-}$ U2OS cells, untreated or treated with 25 ng/ml IL-1β or TNF for 20 minutes. Bar graphs represent results from six independent experiments presented as the mean +/− s.d. *P<0.05, ***P<0,001, ****P<0,0001 (unpaired two-tailed t-test). **c-d,** *S. flexneri* infected HOIP$^{-/-}$ (**c**) and TAK1$^{-/-}$ (**d**) U2OS cells were treated with 25 ng/ml IL-1β for 20 minutes and p65 nuclear translocation was quantified. Bar graphs in **a, c, d** represent results from three independent experiments presented as the mean +/− s.d. *P<0.05, **P<0,01, ***P<0,001, ****P<0,0001 (unpaired two-tailed t-test compared to *ΔipaH1.4/ΔospI* mutant). **e**, Model showing the cooperative action of *Shigella* effectors arrest innate immune signaling during infection. Elimination of M1- and K63-linked ubiquitination by IpaH1.4 and OspI is required for complete suppression of signaling in a cytokine RSC such as IL-1R.